JACS
JOURNAL OF THE AMERICAN CHEMICAL SOCIETY

ARTICLE

pubs.acs.org/JACS

Toward Mechanistic Understanding of Nuclear Reprocessing Chemistries by Quantifying Lanthanide Solvent Extraction Kinetics via Microfluidics with Constant Interfacial Area and Rapid Mixing

Kevin P. Nichols,[‡] Rebecca R. Pompano,[†] Liang Li,[†] Artem V. Gelis,*[,‡] and Rustem F. Ismagilov*[,†]

[†]Department of Chemistry and Institute for Biophysical Dynamics, The University of Chicago, 929 East 57th Street, Chicago, Illinois 60637, United States

[‡]Argonne National Laboratory, 9700 South Cass Avenue, Argonne, Illinois 60439, United States

Supporting Information

ABSTRACT: The closing of the nuclear fuel cycle is an unsolved problem of great importance. Separating radionuclides produced in a nuclear reactor is useful both for the storage of nuclear waste and for recycling of nuclear fuel. These separations can be performed by designing appropriate chelation chemistries and liquid−liquid extraction schemes, such as in the TALSPEAK process (Trivalent Actinide-Lanthanide Separation by Phosphorus reagent Extraction from Aqueous Komplexes). However, there are no approved methods for the industrial scale reprocessing of civilian nuclear fuel in the United States. One bottleneck in the design of next-generation solvent extraction-based nuclear fuel reprocessing schemes is a lack of interfacial mass transfer rate constants obtained under well-controlled conditions for lanthanide and actinide ligand complexes; such rate constants are a prerequisite for mechanistic understanding of the extraction chemistries involved and are of great assistance in the design of new chemistries. In addition, rate constants obtained under conditions of known interfacial area have immediate, practical utility in models required for the scaling-up of laboratory-scale demonstrations to industrial-scale solutions. Existing experimental techniques for determining these rate constants suffer from two key drawbacks: either slow mixing or unknown interfacial area. The volume of waste produced by traditional methods is an additional, practical concern in experiments involving radioactive elements, both from disposal cost and experimenter safety standpoints. In this paper, we test a plug-based microfluidic system that uses flowing plugs (droplets) in microfluidic channels to determine absolute interfacial mass transfer rate constants under conditions of both rapid mixing and controlled interfacial area. We utilize this system to determine, for the first time, the rate constants for interfacial transfer of all lanthanides, minus promethium, plus yttrium, under TALSPEAK process conditions, as a first step toward testing the molecular mechanism of this separation process.

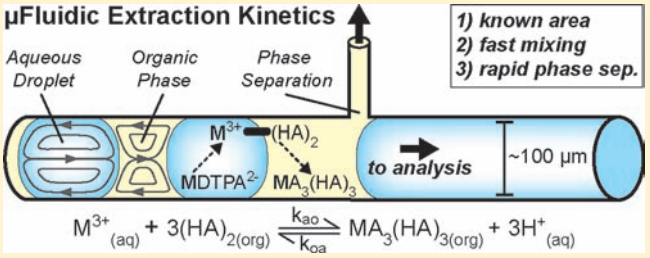

INTRODUCTION

In this paper, we present a microfluidic method to obtain, for the first time, absolute rate constants for two-phase extraction of all stable lanthanide ions relevant to reprocessing used nuclear fuel under the TALSPEAK process (Trivalent Actinide-Lanthanide Separation by Phosphorus reagent Extraction from Aqueous Komplexes) conditions. Over 200 radionuclides are produced during the operation of a typical nuclear reactor.[1] These fission product radionuclides can be chemically separated from used nuclear fuel before recycling and reuse. If the used nuclear fuel is treated as waste after a single use, chemically separating short-lived isotopes from long-lived isotopes would permit a 50-fold greater storage capacity of geological repositories than if the used fuel was immediately disposed of without separation.[2] If the used nuclear fuel is treated as a recyclable material or fuel supply, the fuel must be chemically separated before it can be reused.[3] There are currently no methods approved for industrial-scale reprocessing of civilian nuclear fuel in the United States.[4]

Solvent extraction, in combination with chelation chemistries, is a method of choice for the separation of radionuclides.[5−7] One current bottleneck in the development of next-generation solvent extraction chemistries is the inability to measure the true kinetic rate constants for interfacial mass transfer [cm/s]. While a number of empirical measurements can be performed, the bottleneck is obtaining absolute values of rate constants that are valid independently of the device that is used, that is, with known interfacial area and in a reaction-limited, rapidly mixed regime. Accurate rate constants are needed to elucidate the chemical mechanisms of the extraction processes. In addition, accurate rate constants are needed to predict the efficiency and safety of separation in large-scale industrial systems, in turn impacting both the cost and safety of plant operations.

The TALSPEAK process is under consideration as one component of a multistep system for recycling of used fuels

Received: June 28, 2011
Published: September 02, 2011

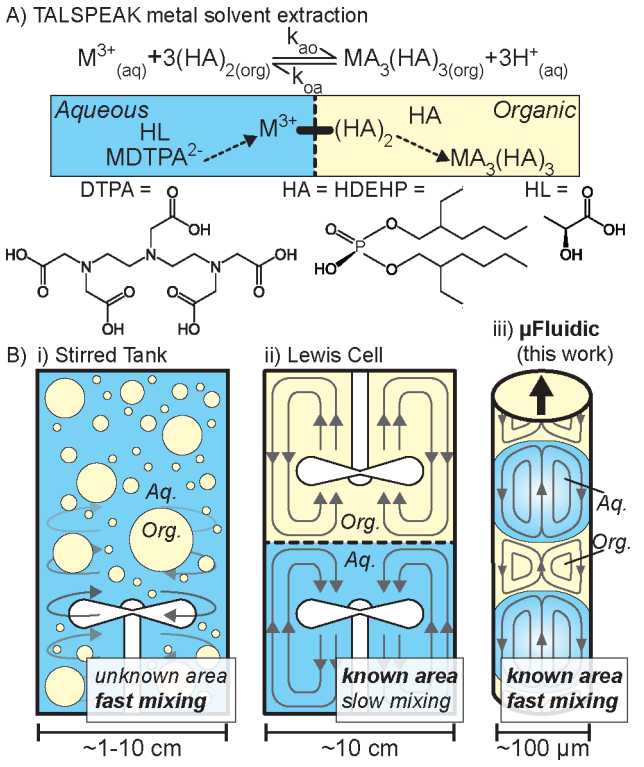

Figure 1. (A) Chemistry of metal-ion separation via solvent extraction under TALSPEAK conditions. The TALSPEAK process is one step in a proposed recycling scheme of nuclear fuel, which separates lanthanides (M^{3+}) from actinides by extracting the lanthanides from an aqueous phase (blue) to an organic phase (yellow). (B) Schematic illustration comparing the traditional methods for measuring kinetics (i,ii) with the method tested here (iii). (i) Highly stirred tanks provide turbulent convective mixing and rapid mixing, but the specific interfacial area is unknown and uncontrolled. (ii) A Lewis cell provides known specific interfacial area ($1-100\ m^{-1}$) with slow diffusive mixing. (iii) Droplet-based microfluidic devices provide rapid mixing, known and large interfacial area ($10\,000\ m^{-1}$), and absolute quantification with high time resolution.

(Figure 1A). Originally described in the 1960s, TALSPEAK is a method for solvent extraction that has been tested on the laboratory scale and is considered to be the most robust process developed to date for separating lanthanides from minor actinides.[5] However, despite decades of research, the precise mechanism of TALSPEAK extraction remains unclear.[8−13] In TALSPEAK, lanthanides are preferentially extracted over actinides from an acidic aqueous solution using a surface-active chelating agent such as bis(2-ethylhexyl) phosphoric acid (commonly abbreviated HDEHP) into an organic phase such as dodecane, while the actinides remain in the aqueous phase complexed with diethylenetriamine-*N*,*N*,*N*′,*N*″,*N*″-pentaacetic acid (DTPA). During the extraction, decomplexation of M-$DTPA^{2-}$ occurs in the aqueous phase, and the free metal ion is transferred to the interface, where the metal ion forms a complex with the dimerized complexing agent HDEHP (HA) and is brought fully into the organic phase as the complex $MA_3(HA)_3$ via ion exchange. DTPA works together with a buffer (either lactic or citric acid), in a currently unknown mechanism, to enhance the selectivity of the extraction, by holding Am^{3+} and Cm^{3+} back in the aqueous phase.

Currently, there are no satisfactory methods to quantify, with known interfacial areas, the rate constants of interfacial mass transfer (i.e., k_{ao} and k_{oa} in Figure 1A) for radioactive species that move slowly across interfaces during solvent extraction. Two types of systems are routinely used to measure the kinetics of solvent extraction and interfacial mass transfer, but they do not necessarily provide data that can provide mechanistic insight, or translate to industrial systems. In addition, both methods use bulk quantities of fluids and therefore can be difficult to use safely with highly radioactive materials, which may require high dilutions, shielding, or even remote operation and are expensive to dispose of as experimental waste.[14] The first system is a highly stirred tank or a vortex mixing system (Figure 1Bi) and is typically analyzed by gamma counting or ICP-MS to determine the metal content of aliquots of each phase. Mixing is rapid, so relative reaction rates can be identified. However, the data are device-specific, interfacial area is unknown and unpredictable, and removing aliquots for analysis affects the specific interfacial area. These tanks also generate large volumes of waste (10−100 mL volumes), so both safety and cost of disposal of experimental waste can be problematic. Because the interfacial area is unknown, it is typically not feasible to carefully vary the experimental conditions to determine the specific reaction mechanism.

The second system commonly used to measure the kinetics of solvent extraction is a Lewis cell (Figure 1Bii), a slow, laminar mixer operated at relatively low Reynolds numbers to maintain a quiescent interface. Lewis cells are typically analyzed by continuous optical or radiometric monitoring and have a known and constant interfacial area. However, the specific interfacial areas that are feasible are small ($1-100\ m^2/m^3$) and result in slow mixing and slow rates of reaction. Processes with small rate constants, such as TALSPEAK, can take days to reach equilibrium in a Lewis cell, but this is the same time scale as the half-lives of some of the radionuclide tracers of interest. Again, safety concerns and disposal costs can be prohibitively high. In addition, only a few cations can be distinguished by continuous monitoring, and only a few lanthanides have characteristic bands in the UV−vis to near-IR range, making Lewis cells impractical for real-time monitoring of realistic mixtures of cations. These systems have a non-negligible diffusion zone, where no active mixing takes place between the two phases. This diffusion zone is typically estimated to be between approximately 50 and 100 μm.[15] It can take 2−20 s for a metal cation to cross via diffusion and significantly longer for ions complexed with extractants. The main problem of slow mixing in this system is that interfacial transfer becomes limited not by intrinsic kinetics, but rather by diffusion of molecules to the interface, and therefore, it becomes impossible to obtain correct rate constants for reactions with rapid transfer kinetics.

Other techniques for measuring rate constants for interfacial mass transfer have also been described in the literature, including moving drops[14] and flow injection analysis.[16] Moving drops are macroscale droplets of one phase that move via the force of gravity through a tank of the other phase. Convection is minimal, and as in a Lewis cell the interfacial area is known but small, leading to slow mixing that limits rates of reaction. The flow injection analysis (FIA) method uses two-phase flow driven through macroscale tubing and junctions. The interfacial surface area can be calculated, but separation of the aqueous and organic phases, for example, through membrane filters, is slow, which severely lowers the temporal resolution. Thus, a method is urgently needed to measure solvent-extraction kinetics with known interfacial area, rapid mixing, high time resolution, and low sample volumes.

Droplet-based microfluidic techniques are well-suited to obtain absolute rate constants for interfacial mass transfer, due to their unique ability to maintain a constant interfacial area while simultaneously achieving rapid mixing. Droplet microfluidics is well-established[17] as a method to quantify chemical kinetics using microliter volumes of sample and has several advantages that make it suitable for the TALSPEAK system. Both fast (millisecond) and slow (hours to days) reactions have been measured,[18−22] and rapid mixing eliminates the effects of diffusion as a confounding factor.[23] Because the interfacial area is known, the results are generalizable, and additional mechanistic insights can be obtained. Additionally, each nanoliter-volume droplet can be considered to be a separate experimental trial, which allows for hundreds or thousands of trials to be performed with just a few microliters of sample. While many droplet-based microfluidic devices have been made in soft elastomers such as PDMS, other materials have also been used to handle harsh chemical systems.[24,25] Microfluidic methods have also been developed both to separate an aqueous phase from an organic phase in a short (subsecond) time frame[26] and to perform the reverse process of phase injection.[27] Rapid, complete isolation of the aqueous phase at a known time point provides high temporal resolution. Microfluidic systems are especially suitable for solvent extraction studies with used nuclear fuel because the small volumes required minimize exposure of lab personnel to radioactive solutions and reduce the high costs of handling and disposing of radioactive waste. Microfluidic systems have also been demonstrated for microscale solvent extraction intended for sample pretreatment or small-scale production purposes.[4,26,28−32]

In this paper, we tested a plug-based microfluidic system that relies on aqueous droplets surrounded by an organic phase to measure absolute rate constants for interfacial mass transfer under TALSPEAK conditions for each metal ion in a model mixture of used nuclear fuel. The device has the mixing speed, large specific interfacial area, and temporal resolution of highly stirred tanks, the control of a Lewis cell, and the rapid and complete phase separation that is unique to microfluidics. We first tested the device by comparing to previously published data obtained in Lewis cells. We further used it to determine, for the first time, the rate constants for 15 elements under TALSPEAK conditions (all lanthanides, minus promethium, plus yttrium) in a first step toward testing the molecular mechanism of the separation process.

RESULTS AND DISCUSSION

Device Design and Characterization. In order to measure the rate constant for interfacial mass transfer in the TALSPEAK system, the device must have three key properties: (1) constant interfacial area (uniform droplet generation); (2) rapid mixing to operate in the "kinetic" regime; and (3) rapid, high purity phase separation. To generate the droplets, we used a flow-focusing geometry[33−35] in laser micromachined tubing with two concentric pieces of FEP tubing (Figure 2i). To separate the aqueous phase from the organic phase at the end of the reactor, we used laser micromachining to create holes in the inner tubing (see Figure S1, Supporting Information). These holes had precise dimensions that were calculated to exclude the aqueous phase and completely separate the organic phase at the applied pressures (Figure 2ii). Details of device fabrication are provided in the Supporting Information (see Experimental Section and Figure S2). A syringe pump controlled the flow rates of organic and aqueous streams into the outer and inner tubing,

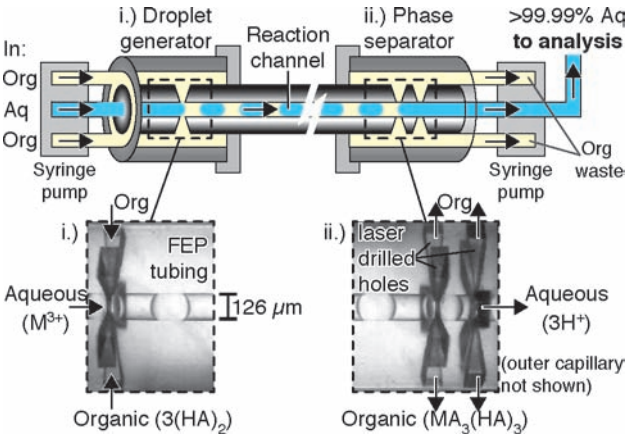

Figure 2. Device design and operation to measure rate constants of interfacial mass transfer in solvent extraction. (top) Schematic showing the design of the device. A single piece of Teflon FEP tubing was micromachined to contain a droplet generator (i), a channel where the extraction occurs (reaction channel), and a phase separator (ii). One syringe pump (left, gray box) is used to control the inflow rates, and a second syringe pump (right, gray box) is used to set the rate of outflow of separated organic phase. The aqueous outflow is collected in aliquots for offline analysis. Additional Swagelok hardware (not shown above but detailed in the Supporting Information) is utilized to properly seal the multiple pieces of tubing and direct the output capillaries from the syringe pump. (bottom) Photos of the regions in the schematic outlined by black dashes show the micromachined holes in the inner FEP tubing: one set of five holes for the droplet generator (i) and two parallel sets of five holes for the phase separator (ii).

respectively. The organic-to-aqueous ratio can be controlled by varying syringe sizes or by using two independent syringe pumps. The flow rate determined the residence time in the system, and varying flow rates allowed multiple contact times to be probed. A second syringe pump was used to set the flow rate of withdrawal from the phase separator; the withdrawn fluid was mostly or purely organic solution. Pure aqueous (>99.99% aqueous) outflow was collected in aliquots from an open outlet for offline analysis. Phase separation was rapid, taking place over less than 300 μm of channel length. Each time point for an experiment that characterized the kinetics of extraction of 1 mM total metal ions (all lanthanides minus promethium, plus yttrium,) in 1 M ammonium citrate, and 0.05 M DTPA, pH = 3.55, with an organic phase of 1 M HDEHP in *n*-dodecane, required 10 μL of collected aqueous phase for ICP-MS analysis, and produced a total of <30 μL of liquid waste (total of aqueous and oil).

Uniform Droplet Generation. Previous work in droplet microfluidics demonstrated that droplets can be generated with regular volumes and that the volumes can be controlled for a wide range of biologically relevant aqueous solutions.[20,36,37] When forming droplets at a T-junction, the volume of the droplet is a function of the capillary number, *Ca*, with three distinct droplet-volume regimes. Therefore, for specific interfacial area, A/V (surface area/volume, mm^2/mm^3), as a function of capillary number, there should be two regimes with constant interfacial area and one regime with a continuously variable interfacial area.[20,37] In this paper, only the constant interfacial area regimes were utilized. However, the variable interfacial area regime could in principle also be utilized, with additional experimental controls.

Solutions used in solvent extraction of lanthanides and actinides contain a variety of surface-active agents such as HDEHP, which could affect the dynamics of droplet formation. To verify that these surface-active agents would not negatively affect

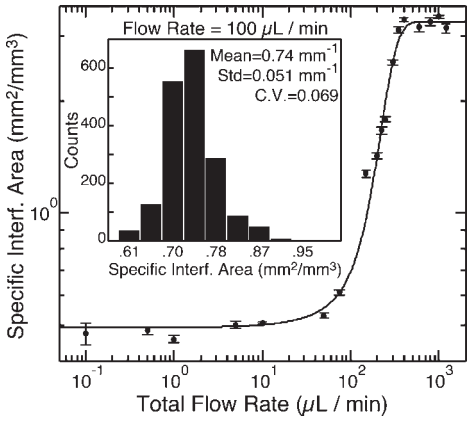

Figure 3. The specific interfacial area of droplets formed in the device is constant for a wide range of flow rates/time points. The graph shows the specific interfacial areas obtained at flow rates for aqueous droplets consisting of 1 mM total metal ions (all lanthanides minus promethium, plus yttrium,), 1 M ammonium citrate, and 0.05 M DTPA, pH = 3.55, in an organic phase of 1 M HDEHP in *n*-dodecane. The organic to aqueous ratio was 1:2. The ambient temperature was 20.0 ± 0.5 °C. The error bars indicate two standard deviations from the mean (N = 15). The fit line is shown to guide the eye. The x-axis shows total inflow rate (aq + org). In the inset bar graph, a computer vision system was used to individually measure the size of 1800 droplets under identical conditions, to determine the specific interfacial area with a greater confidence than can be obtained with the N = 15 measurements. The computer vision system was not utilized at flow rates greater than 100 μL/min due to frame rate limitations.

droplet formation, we first measured the specific interfacial area of droplets composed of these solutions formed in this flow-focusing device over the full range of flow rates required for kinetics experiments (Figure 3). The flow-focusing junction was a series of five 1 μm × 10 μm slits laser machined around the circumference of a 63 μm radius Teflon FEP tube. Droplets were generated at the indicated flow rates and visually inspected under a microscope to ensure that jetting was not occurring. Then the flow was stopped, and droplets were photographed to measure volume. The dependence of interfacial surface area on flow rate was sigmoidal, with the inflection point occurring at $Ca \sim 0.5$, in agreement with previously published results for droplet formation in flow-focusing geometries.[38] For a given flow rate, the droplet volume and therefore the specific interfacial were very regular (Figure 3 inset), with <7% coefficient of variation. All further experiments were carried out in the regime of constant low specific interfacial area, that is, at low flow rates (≤33 μL/min).

Rapid Mixing: Operation in the Kinetic Regime. Analysis of interfacial mass transfer rate constants is greatly simplified when convective mixing is much faster than diffusion to the interface or the rate of interfacial mass transfer. In this case, the rate-limiting process is mass transport across the interface and the system is in the "kinetic" regime as opposed to the "diffusion-limited" regime,[14] enabling measurements of chemically meaningful rate constants. In a Lewis cell (Figure 1Bii), the standard experiment to demonstrate operation in the kinetic regime is to increase the speed of the propeller and measure the rate constant as a function of propeller (mixing) speed. As the mixing speed increases, the rate constant reaches an asymptote where mixing is considered sufficiently faster than diffusion or the reaction of interest.

To achieve rapid mixing in the plug-based microfluidic device, we chose the flow rate, size of the channels, and size of droplets such that convection strongly accelerates diffusive mixing. Mixing is rapid in plug-based microfluidics: the small dimensions result in short diffusion lengths, and the shear forces at the channel walls induce rapid convective recirculation within each droplet and segment of carrier fluid.[39−41] While the microfluidics community sometimes uses the words "plugs" and "droplets" interchangeably, we emphasize that rapid mixing requires plugs (droplets that are pushing against walls of the channel to a sufficient extent to cause recirculation inside the droplet phase[42,43]) and we used plugs for all experiments reported here. For a given channel geometry and molecular diffusion coefficient, the mixing speed is a nonlinear function of flow rate and plug length.[20,39−41] Millisecond-scale mixing is readily achieved in such systems as long as the cross-sectional dimensions are small and can be accelerated by introducing chaotic flows.[18,19] To facilitate rapid mixing, we used tubing with an inner diameter of ∼125 μm and short plug lengths (length/width ratio ∼ 1.5−2). In this device, the analytically predicted mixing time[41] (t_{mix}) ranged from an absolute high of 0.5 s to a low of 0.012 s for flow rates ranging from 1 to 100 μL/min (equations used to generate predictions are detailed in the Supporting Information). As described below, the fastest reactions we measured were ∼5 s (half time of reaction) for La^{3+}, from an aqueous phase with 0.05 M DTPA and 1 M ammonium citrate (pH = 3.55) into an organic phase of 1 M HDEHP in *n*-dodecane at an organic to aqueous ratio of 1:2 and an ambient temperature of 20.0 ± 0.5 °C. Such rapid experiments are performed with shorter residence times at higher flow rates and therefore with faster mixing. This indicates that mixing should not be rate-limiting in our system. To test this prediction experimentally, we compared rate constants (k_{ao}) obtained for extraction of La^{3+} as a function of mixing time. The details of these experimental measurements are described in subsequent sections. We varied mixing time experimentally by varying the flow rate, while varying the length of the reaction channel proportionally to keep the time of reaction constant. As shown in Table 1, we found that the rate constant for interfacial mass transfer, k_{ao}, was the same for all mixing times tested, indicating that our device is operating in the kinetic regime. Thus, the kinetics of interfacial mass transport reactions must indeed be rate-limiting.

Rapid, Pure Phase Separation. The kinetics of extraction of rare earth metals are typically determined by measuring the aqueous metal concentration over time using highly accurate offline analysis methods such as ICP-MS. This method requires isolation of the aqueous phase from the organic phase at a known time point, to prevent further extraction and to obtain an accurate measurement of lanthanide concentration. Recent microfluidic devices have shown excellent phase separation capabilities using long, extended membrane regions,[26] gravity,[28] a "guide structure",[31] or hydrophilic metallic side channels.[44] To achieve rapid, pure phase separation with optimal temporal resolution, here we used an analytical approach that calculated the flow rates and capillary forces necessary to separate the aqueous and organic phases with absolute purity in the shortest period of time (Figure 4).

The system can operate in several regimes of phase purity based on the relative rates of outflow of the siphoned stream (Q_{sip}) and inflow of the aqueous and organic phases (Q_{aq}, Q_{org}) and conservation of volume. When Q_{sip} = 0, all fluid should bypass the withdrawal channel and be collected. In order to siphon all of the organic into the withdrawal channel, Q_{sip} must

Table 1. Measured Rate Constants for Interfacial Mass Transfer of La^{3+} as a Function of Mixing Speed

length of reaction channel (mm)	flow rates range (μL/min)	residence time in reaction channel (s)	predicted t_{mix} (s)	experimental k_{ao} (mm/s), for La^{3+}
317	2.37−118	2−100	0.175−0.012	0.2283 ± 0.0270
185	1.38−69.2	2−100	0.264−0.018	0.2182 ± 0.0077
99	0.741−37.0	2−100	0.450−0.027	0.2381 ± 0.0158
87	0.651−32.5	2−100	0.509−0.029	0.2482 ± 0.0314

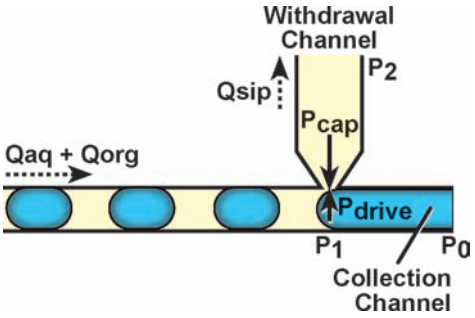

Figure 4. Schematic drawing explaining the physics of phase separation by capillary forces. Droplets of aqueous solution (blue) are moving in organic carrier fluid (yellow). Flow directions (dashed arrows) are indicated for total inflow, $Q_{aq} + Q_{org}$, and controlled outflow of the siphoned organic stream in the withdrawal channel, Q_{sip}. The aqueous sample fluid is collected from the collection channel with an open outlet. The relevant pressures are shown with solid arrows. Siphoning of aqueous solution into the withdrawal channel is regulated by the balance of the driving pressure, $\Delta P_{drive} = (\Delta P_1 - \Delta P_0) - (\Delta P_1 - \Delta P_2)$, against the capillary pressure at the entry to the withdrawal channel, ΔP_{cap}.

be greater than or equal to Q_{org}. If $Q_{sip} > Q_{org}$, some aqueous solution will also be siphoned along with the organic. Perfect separation of organic and aqueous is possible in principle only if $Q_{sip} = Q_{org}$, but this flow condition is not sufficient to provide separation. When $Q_{sip} = Q_{org}$, the balance of capillary pressure at the entry to the withdrawal channel (ΔP_{cap}, [Pa]) and the driving pressure ($\Delta P_{drive} = (\Delta P_1 - \Delta P_0) - (\Delta P_1 - \Delta P_2)$, [Pa]) determines whether aqueous is siphoned along with organic.

To predict the conditions under which the aqueous is excluded from the withdrawal channel, we adapted a previously published description of capillary pressure and driving pressure in microfluidic devices.[26,45] The aqueous droplet is prevented from entering the withdrawal channel by capillary pressure, ΔP_{cap}, at the entrance:

$$\Delta P_{cap} = -2\gamma \cos\theta \left(\frac{1}{R_o}\right) \quad (1)$$

where γ is the aq−org interfacial surface tension [N/m], θ is the contact angle of the aqueous droplet on the surface of the device in the bulk organic phase [radians], and R_o is the radius of curvature [m] of the opening into the withdrawal channel.

The aqueous droplet is driven into the withdrawal channel by a driving pressure, ΔP_{drive}, which opposes ΔP_{cap}. The driving pressure is the pressure difference between a positive pressure due to flow resistance downstream in the main channel ($\Delta P_1 - \Delta P_0$) and a negative pressure set by withdrawing syringe pump ($\Delta P_1 - \Delta P_2$). ΔP_i refers to gauge pressure (pressure above ambient atmosphere) at position P_i (see Figure 4 for positions). If the main tubing is open to the atmosphere, then ΔP_0 is zero, and thus for a cylindrical channel such as is used here:

$$(\Delta P_1 - \Delta P_0) = \frac{8\mu_{aq} L_1 (Q_{org} + Q_{aq} - Q_{sip})}{\pi {R_1}^4} \quad (2)$$

where μ_{aq} is the viscosity of aqueous phase [Pa·s] and L_1 and R_1 are the length [m] and radius [m], respectively, of the main tubing downstream from the siphon point. The withdrawing pump sets the negative pressure in the withdrawal channel by controlling the outflow rate $Q_{sip} > 0$, such that

$$(\Delta P_1 - \Delta P_2) = -\frac{8(f_{org}\mu_{org} + f_{aq}\mu_{aq}) L_2 (Q_{sip})}{\pi {R_2}^4} \quad (3)$$

where μ_{org} is the viscosity of organic phase [Pa·s], f_i is the fraction of siphoned fluid consisting of phase i, and L_2 and R_2 are the length [m] and radius [m], respectively, of the withdrawal channel. During perfect separation, only the organic phase is siphoned, so $f_{org} = 1$ and $f_{aq} = 0$. The driving pressure is given by the difference between these terms:

$$\Delta P_{drive} = (\Delta P_1 - \Delta P_0) - (\Delta P_1 - \Delta P_2) \quad (4)$$

In the regime $Q_{sip} \leq Q_{org}$, this analysis predicts that the aqueous stream could be excluded from the withdrawal channel if and only if $\Delta P_{drive} < \Delta P_{cap}$; otherwise, both aqueous and organic would be siphoned. The maximum size of the opening of the withdrawal channel predicted to provide perfect separation was found by equating eqs 1 and 4 and solving for R_o when $Q_{sip} = Q_{org}$:

$$R_o = \frac{-2\gamma \cos\theta}{\left(\frac{8\mu_{aq} L_1 Q_{aq}}{\pi {R_1}^4} + \frac{8\mu_{org} L_2 Q_{sip}}{\pi {R_2}^4}\right)} \quad (5)$$

We used the dimensions of our device and the properties of the aqueous and organic solutions used for subsequent extraction experiments (see Fluid Properties and Table S1 in the Supporting Information) to predict the maximum size of the opening that would provide perfect separation. For flow rates up to $Q_{sip} = Q_{org} = 100\ \mu$L/min, we found that the critical R_o was ~1 μm. We utilized this dimension as a fabrication target for laser micromachining.

We tested the accuracy of the predictions for separation of the aqueous and organic phases by quantifying the composition of the stream exiting the collection channel as a function of the inflow and outflow rates (Figure 5). The dimensions of the device are given in Table S1 in the Supporting Information. The device had 10 exit holes for phase separation fabricated by an excimer laser (as shown in Figure 2ii), each with ~1 μm × 10 μm rectangular cross sections at the tip where they contacted the lumen of the extraction channel. Phase separation was characterized using flow rates that would produce residence times between 0.5 s and 1 min. In our 88 mm long reaction channel with an inner

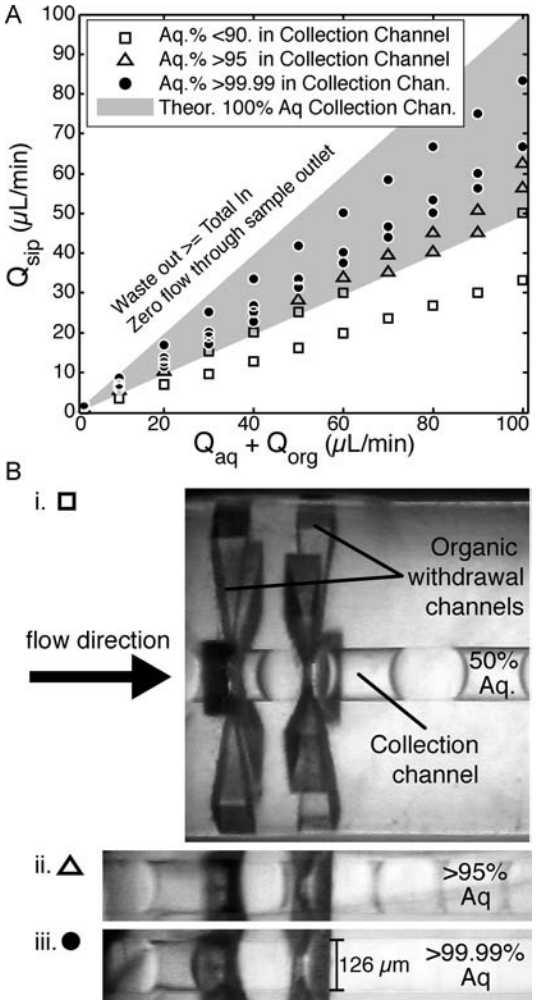

Figure 5. Characterization of purity of the collected aqueous stream after phase separation and comparison to theoretical predictions. (A) Phase diagram showing the composition of the collected sample stream (aqueous collected volume/total collected volume) as a function of inlet and withdrawal channel flow rates. The inlet rate shown corresponds to total fluid inflow ($Q_{org} + Q_{aq}$). Experimental data was obtained with droplets of an aqueous solution of a mixture of 14 lanthanides and yttrium (each at 1 mM) with 1 M ammonium citrate and 0.05 M DTPA (pH = 3.55) in a carrier fluid of 1 M HDEHP in dodecane. Organic to aqueous ratio was 1:1. Ambient temperature was 20.0 ± 0.5 °C. (B) Photos of the device during use at three different inlet/outlet ratios, resulting in (i) zero flow through the phase separation channels, that is, 50% aqueous in the sample outflow; (ii) >95% aqueous in the sample outflow; and (iii) >99.9% aqueous in the sample outflow. The device consisted of 10 phase separation channels; two rows of 5 radially arranged phase separation channels are visible in the photos, each with an ~1 μm × 10 μm cross section at the narrow end. Scale is the same for all photos.

radius of 63 μm, this corresponded to flow rates between 1 and 100 μL/min.

As expected, with an outflow rate of zero ($Q_{sip} = 0$), both the aqueous and organic phases bypassed the separation channels and exited the system (Figure 5Bi). For $Q_{sip} > (Q_{aq} + Q_{org})$, all fluid was siphoned and no flow was observed through the sample outlet. These results agree with conservation of volume and indicated that dead volumes were small or negligible in the device. Perfect separation was predicted to occur at $Q_{sip} = Q_{org}$

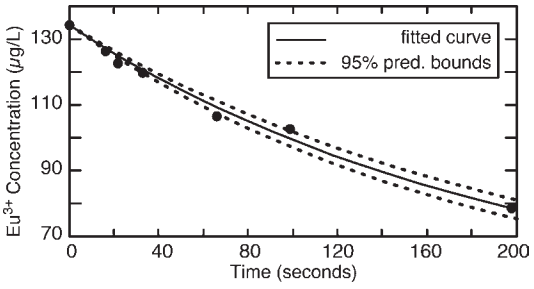

Figure 6. Primary concentration versus time data for extraction obtained using the tested device under conditions that duplicated previously published results:[46] the aqueous phase initially contained Eu^{3+} at 134 μg/L and 0.05 M HEDTA, 1 M NaCl, 0.2 mM lactic acid at a p[H] of 3.00. The organic to aqueous volumetric ratio was 1:1. The ambient temperature was 20.0 ± 0.5 °C. The decay shows the transfer into an organic phase containing 0.01 M HDEHP in dodecane. Circles indicate primary data points obtained using the tested method and ICP-MS. The curves are fit using eq 7. Prediction bounds were calculated using the predint function in MATLAB 7.6 and indicate the upper and lower 95% prediction bounds for the fitted curve.

(Figure 5A) when the entry to the withdrawal channel is restricted to $R_o \sim 1$ μm as discussed above. Although the aqueous stream was successfully excluded from the withdrawal channel at $Q_{sip} \leq Q_{org}$, we found that, at $Q_{sip} = Q_{org}$, the aqueous stream in the collection channel still contained some of the organic phase. A higher outflow rate, $Q_{sip} \geq 1.3(Q_{org})$, was required for the collection channel to have an aqueous stream with >99.99% purity (Figure 5A, black circles; also Figure 5Biii). There are several potential factors, not included in the model, which may be responsible for imperfect agreement between theory and experiment: (i) additional resistance terms, such as flow through the narrow laser-drilled inlets to the withdrawal channels; (ii) additional capillary pressure produced by droplets of aqueous solution that were siphoned into the withdrawal channel; and (iii) imperfect control of the dimensions of the 1 × 10 μm^2 opening, which is at the limit of the capabilities for excimer laser machining in soft materials. Yet, the agreement was sufficiently good that we could confidently design devices and carry out kinetic measurements. Conservation of volume predicts that some aqueous solution would be siphoned into the withdrawal channel at these flow rates, so the withdrawn organic stream was not pure. Nevertheless, because the kinetics of extraction were analyzed by measuring the lanthanide concentration in the aqueous stream, as long as the capillary pressure was sufficient to provide a pure aqueous stream, kinetic data was easily obtained.

Quantifying Kinetics of Solvent Extraction. After verifying that the device could provide rapid, pure phase separation, we used the device to determine the concentration of lanthanide ions in the aqueous phase, C, versus time during extraction (see Experimental Section in the Supporting Information for additional details). All experiments, except those specifically designed to test the effects of mixing channel length, were carried out in 88 mm long tubing with an internal radius of 63 μm. In this 88 mm long tubing, different flow rates were utilized to set different residence times, and the final concentrations in the aqueous phase were individually plotted. Typically, 15 points were taken to cover the range from ~2 to ~450 s, with the majority of the points taken toward the beginning of the experiment. For example, Figure 6 shows the transfer of Eu^{3+} from an aqueous

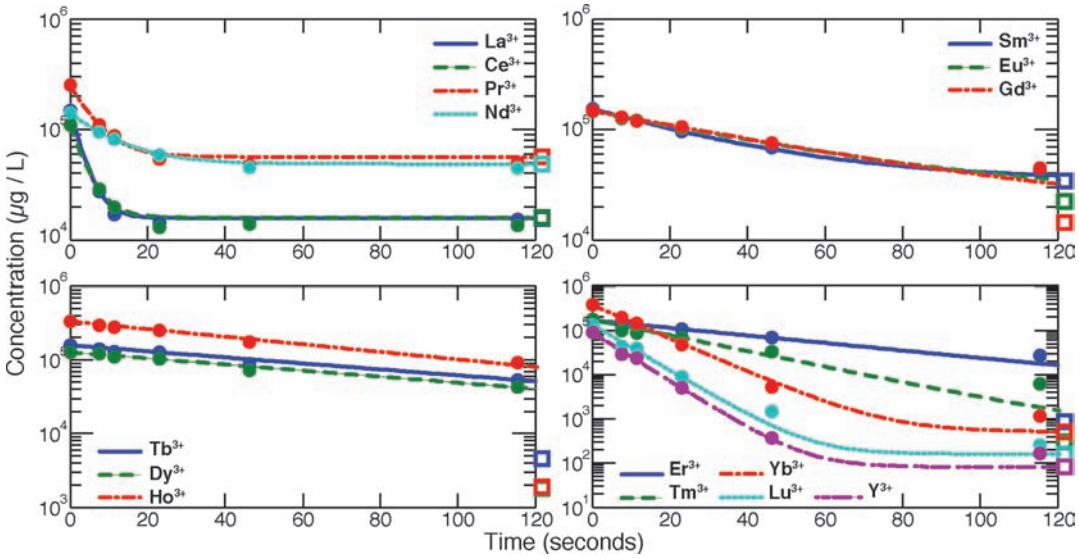

Figure 7. Plots of concentration versus time for extraction obtained using the tested device under TALSPEAK conditions: the aqueous phase was 0.05 M DTPA and 1 M ammonium citrate (pH = 3.55); the organic phase was 1 M HDEHP in *n*-dodecane. Organic to aqueous ratio was 1:2. The ambient temperature was 20.0 ± 0.5 °C. The first 120 s of primary data is plotted. This data was used to obtain the constants in Table 2, plotted in Figure 8. Circles indicate primary data points obtained using the tested device and ICP-MS. Squares indicate equilibrium points, obtained via test tube experiments and identical ICP-MS processing. The curves were fit using eq 7.

phase (0.05 M (2-hydroxyethyl)ethylenediamine-*N*,*N*,*N*′ -triacetic acid (HEDTA), 1 M NaCl, 0.2 mM lactic acid, p[H] 3.00) into an organic phase containing 0.01 M HDEHP in dodecane. The organic to aqueous ratio was 1:1. The ambient temperature was 20.0 ± 0.5 °C. A volume of 10 μL of aqueous solution was collected for each data point. Since each aqueous droplet is approximately 2 nL, this 10 μL sample represents approximately 5000 individual trials averaged together.

All data were analyzed according to a first order decay equation for the equilibrium $C \rightleftharpoons C_{org}$, with forward and backward interfacial mass transfer rate constants k_{ao} and k_{oa}, respectively, distribution ratio $K_D = k_{ao}/k_{oa} = C_{org,eq}/C_{eq}$, and initial aqueous concentration C_0. Assuming that $C_{org} = 0$ initially and that there are no side reactions to consume the aqueous metal ions, the rate equation is

$$dC/dt = (A/V)(k_{oa}C_{org} - k_{ao}C) \quad (6)$$

Integration over t from 0 to t and over C from C_0 to C gives[47,48]

$$\frac{C_{eq} - C}{C_{eq} - C_0} = e^{-k_{oa}(A/V)(1 + (V_{org}/V_{aq})K_D)t} \quad (7)$$

Here, V_{org}/V_{aq} is the ratio of the volumetric flow rate of the organic phase to the aqueous phase. Concentration versus time data from experiments was fit according to eq 7, and 95% prediction intervals were plotted (Figure 6). All parameters except k_{oa} [mm/s] are known from independent experimental measurements (see Experimental Section in the Supporting Information); therefore, k_{oa} can be determined by fitting the data to eq 7. From the fitted k_{oa} and known K_D, we solved for the forward interfacial mass transfer rate constant k_{ao} [mm/s]

$$k_{ao} = k_{oa}K_D \quad (8)$$

The device-independent interfacial mass transfer rate constants are multiplied by the specific interfacial area A/V [1/mm] to obtain the device-specific rate of interfacial mass transfer [1/s].

First, we tested whether the device produced data that was consistent with results obtained by traditional methods. We used the device to measure the kinetics of extraction of europium ions ($C_0 = 1\ \mu$M) from the aqueous phase (0.05 M HEDTA, 1 M NaCl, 0.2 mM lactic acid, p[H] 3.00) by 0.01 M HDEHP in dodecane (Figure 6). k_{ao} was determined to be $9.1 \times 10^{-5} \pm 0.8 \times 10^{-5}$ cm/s, and k_{oa} was $4.7 \times 10^{-5} \pm 2.2 \times 10^{-5}$ cm/s; the literature value, extracted from a graph, of k_{ao} for this extraction was 3×10^{-5} cm/s.[46] The literature value was obtained using a centimeter-scale Lewis cell; contemporaneous modeling[15] predicted that a 60 μm diffusion zone was located in the center of that device. Each droplet in the two-phase system tested here was only ~160 μm long under tested conditions and 125 μm wide, with rapid internal mixing. We would therefore expect to find a higher k_{ao} than measured previously by constant interfacial area cells.

Next, we used the device to test the kinetics of extraction of a mixture of yttrium and the full series of stable lanthanides under TALSPEAK conditions. C_0 of each cation was 0.01 mM (0.15 mM total metal ion) in 0.05 M DTPA and 1 M ammonium citrate (pH = 3.55); the organic phase was 1 M HDEHP in *n*-dodecane. The ambient temperature was 20.0 ± 0.5 °C. The organic to aqueous ratio was 1:2. The collected aqueous sample stream was analyzed at each time point using ICP-MS to quantify all cations simultaneously (Figure 7), and interfacial mass transport rate constants were determined for each cation (Figure 8, Table 2). The true rate constant should be independent of the initial concentration of lanthanides. We verified that the rate constants remained the same after decreasing the concentration of each cation 10-fold to 0.015 mM (Figure 8). These results indicated that Dy^{3+} has the slowest extraction kinetics under the TALSPEAK conditions tested.

In a mixture of cations, the components could interfere with one another, for example, if more rapidly extracted cations

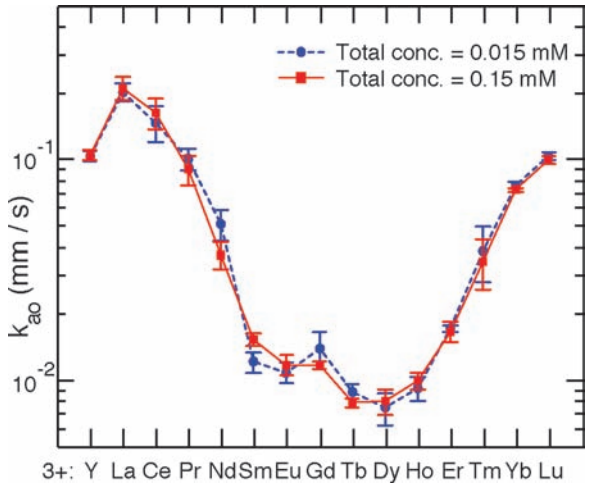

Figure 8. Kinetic data obtained using the device under TALSPEAK conditions. C_0 of each cation was either 0.01 mM (red squares) or 0.001 mM (blue circles) in 0.05 M DTPA and 1 M ammonium citrate (pH = 3.55); the organic phase was 1 M HDEHP in *n*-dodecane. The organic to aqueous ratio was 1:2. The ambient temperature was 20.0 ± 0.5 °C. A plot of the k_{ao} was obtained from each regression for each cation. The error bar on each k_{ao} indicates the 95% confidence interval. Error bars were calculated from single experiments (Figure 7), and they indicate the confidence interval calculated based upon the deviation from the fit to individual measurements of concentration versus time. Such error bars were determined in MATLAB 7.6 using the inverse R factor from the QR decomposition of the Jacobian, the degrees of freedom for error, and the root mean squared error. Table 2 presents k_{ao} and k_{oa} values corresponding to the red curve.

Table 2. Kinetics Obtained Using the Device under TALSPEAK Conditions, for the Conditions Shown as a Graph in Figure 8[a]

cation	k_{ao} (mm/s)	k_{oa} (mm/s)
Y	$1.0 \times 10^{-1} \pm 5.5 \times 10^{-3}$	$1.9 \times 10^{-4} \pm 1.0 \times 10^{-5}$
La	$2.1 \times 10^{-1} \pm 2.6 \times 10^{-2}$	$5.0 \times 10^{-2} \pm 6.1 \times 10^{-3}$
Ce	$1.6 \times 10^{-1} \pm 2.6 \times 10^{-2}$	$5.5 \times 10^{-2} \pm 8.8 \times 10^{-3}$
Pr	$9.0 \times 10^{-2} \pm 1.4 \times 10^{-2}$	$5.2 \times 10^{-2} \pm 7.9 \times 10^{-3}$
Nd	$3.7 \times 10^{-2} \pm 5.3 \times 10^{-3}$	$3.9 \times 10^{-2} \pm 5.6 \times 10^{-3}$
Sm	$1.5 \times 10^{-2} \pm 9.6 \times 10^{-4}$	$8.7 \times 10^{-3} \pm 5.5 \times 10^{-4}$
Eu	$1.2 \times 10^{-2} \pm 1.3 \times 10^{-3}$	$4.2 \times 10^{-3} \pm 4.5 \times 10^{-4}$
Gd	$1.2 \times 10^{-2} \pm 4.7 \times 10^{-4}$	$2.5 \times 10^{-3} \pm 1.0 \times 10^{-4}$
Tb	$7.8 \times 10^{-3} \pm 3.8 \times 10^{-4}$	$4.6 \times 10^{-4} \pm 2.2 \times 10^{-5}$
Dy	$7.9 \times 10^{-3} \pm 1.1 \times 10^{-3}$	$2.3 \times 10^{-4} \pm 3.1 \times 10^{-5}$
Ho	$9.9 \times 10^{-3} \pm 8.6 \times 10^{-4}$	$1.1 \times 10^{-4} \pm 9.9 \times 10^{-6}$
Er	$1.6 \times 10^{-2} \pm 1.7 \times 10^{-3}$	$1.7 \times 10^{-4} \pm 1.7 \times 10^{-5}$
Tm	$3.4 \times 10^{-2} \pm 8.9 \times 10^{-3}$	$1.2 \times 10^{-4} \pm 3.1 \times 10^{-5}$
Yb	$7.2 \times 10^{-2} \pm 1.7 \times 10^{-3}$	$1.9 \times 10^{-4} \pm 4.5 \times 10^{-6}$
Lu	$9.9 \times 10^{-2} \pm 3.8 \times 10^{-3}$	$2.3 \times 10^{-4} \pm 8.8 \times 10^{-6}$

[a] C_0 of each cation was 0.01 mM in 0.05 M DTPA and 1 M ammonium citrate, pH = 3.55; the organic phase was 1 M HDEHP in *n*-dodecane. The organic to aqueous ratio was 1:2. The ambient temperature was 20.0 ± 0.5 °C.

dominate the available interfacial HDEHP binding sites, thereby slowing the extraction of other cations. We tested whether interference affected the kinetics observed in the device by measuring the interfacial mass transfer rate constant of the metal ions with the lowest rate constant, Dy^{3+}, alone instead of in a mixture. C_0 of each cation was 0.01 mM in 0.05 M DTPA and 1 M ammonium citrate (pH = 3.55); the organic phase was 1 M HDEHP in *n*-dodecane. The organic to aqueous ratio was 1:2. The ambient temperature was 20.0 ± 0.5 °C. We found the rate constant was unchanged (Table 3); therefore, cation interference is not a significant effect in this system, as expected from the high HDEHP/metal ion molar ratio.

Table 3. Interfacial Mass Transfer Rate Constants for Dysprosium in a Mixture of 14 Other Metal Cations and without Additional Metal Cations[a]

	k_{ao} (mm/s)
Dy^{3+} (in lanthanide mixture)	0.0083 ± 0.0016
Dy^{3+} (without lanthanide mixture)	0.0091 ± 0.0010

[a] Error bars were calculated after nonlinear regression to eq 7 and indicate the confidence interval calculated based upon the deviation from the fit to individual measurements.

CONCLUSION

Here, we have tested a microfluidic method to measure the kinetics of metal ion extraction under conditions that are in development for separation of streams of used nuclear fuel. This device, for the first time, measured individual absolute interfacial mass transport rate constants for 15 nuclides extracted from a mixture while surface area, mixing rate, and other parameters were under total control. Furthermore, the high specific interfacial area enabled rapid rates of reaction, which is especially valuable for reactions with high rate constants because (i) it allows measurement of the extent of reaction from short contact times to equilibrium; and (ii) the measurement of true rate constants was not obscured by mixing limitations. For a series of experiments such as those in Figures 7 and 8, each time point required 10 μL of aqueous phase for ICP-MS analysis (which produced data for all metal ions at each time point) and produced a total of less than 30 μL of liquid waste (total of aqueous and organic), therefore addressing the significant experimental radiation safety concerns.

The data obtained by this method revealed unexpected kinetic information that is relevant to mechanistic insight and industrial models of the TALSPEAK process. We observed that Dy^{3+} has the slowest extraction kinetics under the TALSPEAK conditions, and that the heavier lanthanides are actually extracted faster under the tested conditions. Previously, it was believed that the extraction rate slows down as the lanthanide atomic number increases,[49] but the heavy lanthanides (beyond Gd) were not probed in previous studies. The extraction mechanism of TALSPEAK includes several steps that could affect the overall rate of interfacial mass transfer, such as decomplexation of the Ln−DTPA complex, transfer of Ln^{3+} to the interface (believed to be rapid in the device tested here), and multistep formation of the Ln−HDEHP complex in the organic phase.[14] The buffer (here citrate, though lactate is commonly used as well) may also play a role in determining the rate of extraction, which requires further investigation. Further mechanistic understanding and optimization of TALSPEAK chemistry and its analogues will be greatly enhanced by this methodology, facilitating reprocessing of nuclear waste with the potential to address a problem of significance to energy, environment, and national security.

■ ASSOCIATED CONTENT

Supporting Information. Experimental details, additional figures and tables, and complete refs 6 and 7. This material is available free of charge via the Internet at http://pubs.acs.org

■ AUTHOR INFORMATION

Corresponding Author
r-ismagilov@uchicago.edu; guelis@anl.gov

■ ACKNOWLEDGMENT

This work was supported by the U.S. Department of Energy, Office of Nuclear Energy, Fuel Cycle Research and Development Project under Contract DE-AC02-06CH11357. We thank Heidi Park for contributions to writing and editing this manuscript.

■ REFERENCES

(1) Crowley, K. D. *Phys. Today* **1997**, *50*, 32–39.
(2) Todd, T. A.; Wigeland, R. A. In *Separations for the Nuclear Fuel Cycle in the 21st Century*; Lumetta, G. J., Nash, K. L., Clark, S. B., Friese, J. I., Eds.; American Chemical Society: Washington, DC, 2006; Vol. 933, pp 41−55.
(3) Fukasawa, T.; Yamashita, J.; Hoshino, K.; Fujimura, K.; Sasahira, A. *Proceedings of 16th International Conference on Nuclear Engineering (ICONE16)*, Orlando, FL, May 11−15 2008; ASME: New York, 2008; ICONE16-48567; pp 105−109.
(4) Andrews, A. *Nuclear Fuel Reprocessing: US Policy Development*; Congressional Research Service: Washington, DC, 2006.
(5) Gelis, A. V.; Vandegrift, G. F.; Bakel, A.; Bowers, D. L.; Hebden, A. S.; Pereira, C.; Regalbuto, M. *Radiochim. Acta* **2009**, *97*, 231–232.
(6) Vandegrift, G. F. et al. Designing and Demonstration of the UREX+ Process Using Spent Nuclear Fuel. Presented at *Advances for Future Nuclear Fuel Cycles International Conference*, Nimes, France, June 21−24, 2004; Paper 012-01.
(7) Vandegrift, G. F. et al. Lab Scale Demonstration of the UREX+ Process. In *Waste Management '04 Conference,* Tucson, AZ, February 29−March 4, 2004; Paper WM-4323.
(8) Nash, K. L. *Solvent Extr. Ion Exch.* **1993**, *11*, 729–768.
(9) Nash, K. L. *Key features of the TALSPEAK and similar trivalent actinide-lanthanide partitioning processes*; Chemical Sciences Division, Oak Ridge National Laboratory: Oak Ridge, TN, 2008.
(10) Nilsson, M.; Nash, K. L. *Solvent Extr. Ion Exch.* **2007**, *25*, 665–701.
(11) Nilsson, M.; Nash, K. L. *Solvent Extr. Ion Exch.* **2009**, *27*, 354–377.
(12) Grimes, T. S.; Nilsson, M.; Nash, K. L. *The behavior and importance of lactic acid complexation in Talspeak extraction systems*; Chemical Sciences Division, Oak Ridge National Laboratory: Oak Ridge, TN, 2008.
(13) Zalupski, P. R.; Nash, K. L.; Nakamura, Y.; Yamamoto, M.; Martin, L. R. *IOP Conf. Ser.: Mater. Sci. Eng.* 2010, *9*, 012076.
(14) Danesi, P. R.; Chiarizia, R.; Coleman, C. *Crit. Rev. Anal. Chem.* **1980**, *10*, 1–126.
(15) Danesi, P. R.; Vandegrift, G. F.; Horwitz, E. P.; Chiarizia, R. *J. Phys. Chem.* **1980**, *84*, 3582–3587.
(16) Kubán, V. *Crit. Rev. Anal. Chem.* **1991**, *22*, 477–477.
(17) Song, H.; Chen, D. L.; Ismagilov, R. F. *Angew. Chem., Int. Ed.* **2006**, *45*, 7336–7356.
(18) Bringer, M. R.; Gerdts, C. J.; Song, H.; Tice, J. D.; Ismagilov, R. F. *Philos. Trans. R. Soc. A* **2004**, *362*, 1087–1104.
(19) Song, H.; Bringer, M. R.; Tice, J. D.; Gerdts, C. J.; Ismagilov, R. F. *Appl. Phys. Lett.* **2003**, *83*, 4664–4666.
(20) Tice, J. D.; Song, H.; Lyon, A. D.; Ismagilov, R. F. *Langmuir* **2003**, *19*, 9127–9133.
(21) Song, H.; Li, H. W.; Munson, M. S.; Van Ha, T. G.; Ismagilov, R. F. *Anal. Chem.* **2006**, *78*, 4839–4849.
(22) Chen, D. L.; Gerdts, C. J.; Ismagilov, R. F. *J. Am. Chem. Soc.* **2005**, *127*, 9672–9673.
(23) Song, H.; Ismagilov, R. F. *J. Am. Chem. Soc.* **2003**, *125*, 14613–14619.
(24) Kreutz, J. E.; Shukhaev, A.; Du, W.; Druskin, S.; Daugulis, O.; Ismagilov, R. F. *J. Am. Chem. Soc.* **2010**, *132*, 3128–3132.
(25) Begolo, S.; Colas, G.; Viovy, J. L.; Malaquin, L. *Lab Chip* **2011**, *11*, 508–512.
(26) Kralj, J. G.; Sahoo, H. R.; Jensen, K. F. *Lab Chip* **2007**, *7*, 256–263.
(27) Li, L.; Boedicker, J. Q.; Ismagilov, R. F. *Anal. Chem.* **2007**, *79*, 2756–2761.
(28) Kralj, J. G.; Schmidt, M. A.; Jensen, K. F. *Lab Chip* **2005**, *5*, 531–535.
(29) Kreutzer, M. T.; Gunther, A.; Jensen, K. F. *Anal. Chem.* **2008**, *80*, 1558–1567.
(30) Mary, P.; Studer, V.; Tabeling, P. *Anal. Chem.* **2008**, *80*, 2680–2687.
(31) Priest, C.; Zhou, J.; Sedev, R.; Ralston, J.; Aota, A.; Mawatari, K.; Kitamori, T. *Int. J. Miner. Process.* **2011**, *98*, 168–173.
(32) Silvestre, C. I. C.; Santos, J. L. M.; Lima, J. L. F. C.; Zagatto, E. A. G. *Anal. Chim. Acta* **2009**, *652*, 54–65.
(33) Abate, A. R.; Thiele, J.; Weitz, D. A. *Lab Chip* **2011**, *11*, 253–258.
(34) Anna, S. L.; Bontoux, N.; Stone, H. A. *Appl. Phys. Lett.* **2003**, *82*, 364–366.
(35) Utada, A. S.; Lorenceau, E.; Link, D. R.; Kaplan, P. D.; Stone, H. A.; Weitz, D. A. *Science* **2005**, *308*, 537–541.
(36) Teh, S. Y.; Lin, R.; Hung, L. H.; Lee, A. P. *Lab Chip* **2008**, *8*, 198–220.
(37) Tice, J. D.; Lyon, A. D.; Ismagilov, R. F. *Anal. Chim. Acta* **2004**, *507*, 73–77.
(38) Abate, A. R.; Poitzsch, A.; Hwang, Y.; Lee, J.; Czerwinska, J.; Weitz, D. A. *Phys. Rev. E* 2009, *80*, 026310-1–026310-5.
(39) Handique, K.; Burns, M. A. *J. Micromech. Microeng.* **2001**, *11*, 548–554.
(40) Kashid, M. N.; Gerlach, I.; Goetz, S.; Franzke, J.; Acker, J. F.; Platte, F.; Agar, D. W.; Turek, S. *Ind. Eng. Chem. Res.* **2005**, *44*, 5003–5010.
(41) Rhee, M.; Burns, M. A. *Langmuir* **2008**, *24*, 590–601.
(42) King, C.; Walsh, E.; Grimes, R. *Microfluid. Nanofluid.* **2007**, *3*, 463–472.
(43) Song, H.; Chen, D. L.; Ismagilov, R. F. *Angew. Chem., Int. Ed.* **2006**, *45*, 7336–7356.
(44) Scheiff, F.; Mendorf, M.; Agar, D.; Reis, N.; Mackley, M. *Lab Chip* **2011**, *11*, 1022–1029.
(45) Li, L.; Karymov, M. A.; Nichols, K. P.; Ismagilov, R. F. *Langmuir* **2010**, *26*, 12465–12471.
(46) Danesi, P. R.; Cianetti, C. *Sep. Sci. Technol.* **1982**, *17*, 969–969.
(47) Danesi, P. R.; Vandegrift, G. F. *J. Phys. Chem.* **1981**, *85*, 3646–3651.
(48) Ting, H. P.; Bertrand, G. L.; Sears, D. F. *Biophys. J.* **1966**, *6*, 813–823.
(49) Kolarik, Z.; Koch, G.; Kuhn, W. *J. Inorg. Nucl. Chem.* **1974**, *36*, 905–909.